CHAPTER

ICE CAVES IN AUSTRIA

13

Christoph Spötl*, Maximilian Wimmer†, Rudolf Pavuza‡, Lukas Plan‡

University of Innsbruck, Innsbruck, Austria Landesverein für Höhlenkunde in Oberösterreich, Linz, Austria† Natural History Museum Vienna, Vienna, Austria‡*

CHAPTER OUTLINE

13.1 INTRODUCTION

Austria is located in central Europe and comprises 29% of the Alps, also known as Eastern Alps. The high proportion of mountainous terrain reaching up to 3798 m a.s.l.—65% of the country's size—and the widespread distribution of karstifiable carbonate rocks (and in particular the presence of large uplifted karst plateaus) are the main reasons for the high abundance of ice-bearing caves in this country. The number of ice caves relative to the size of the country probably ranks among the highest worldwide.

About one fifth of Austria is made up of carbonate rocks, ranging from non-metamorphic limestones and dolomites to low- and medium-grade metamorphic marbles and calcareous schists. Although karst caves constitute by far the longest and deepest caves, caves unrelated to karst processes are also quite common in some regions, but few host cave ice.

16,300 caves are known and registered in the national cave cadaster (as of December 2016). They are unevenly distributed across the country, showing the highest abundance and density in the central and eastern segments of the Northern Calcareous Alps (NCA), as well as in the area north and northwest of Graz (Fig. 13.1).

Ice Caves. https://doi.org/10.1016/B978-0-12-811739-2.00013-9

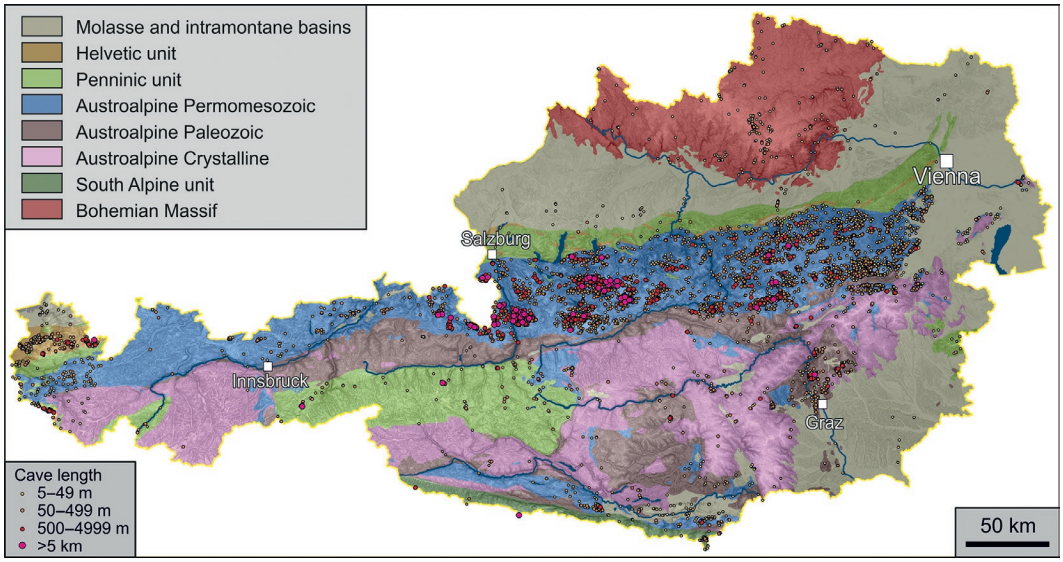

FIG. 13.1

Simplified geological map of Austria showing the distribution of caves as of 2017.

Schönberghöhlensystem, located in the western part of Totes Gebirge, is the longest cave in the European Union and comprises 146.7 km of passages (see below). Two additional caves are longer than 100 km, and 14 more caves exceed 20 km. Sixteen caves in Austria are deeper than 1 km, which reflects the thick vadose zone of uplifted karst massifs. Lamprechtsofen ranks as the deepest through-trip cave worldwide, with a vertical extent of 1632 m between the lower and the highest-lying entrance.

Thanks to the centralized cave cadaster operated by a web-based database system (Spelix), in which speleologists from 26 local caving clubs feed their exploration data, Austria has a comprehensive and well-maintained database of caves, including ice-bearing ones. 1200 caves classify as ice caves that host perennial ice, firn, or snow. Less well known is the temporal evolution of these caves, but qualitative observations clearly indicate that a number of ice-bearing caves has partly or completely lost their ice deposits in the past few decades.

13.2 ICE CAVE RESEARCH

Research on ice in subsurface cavities has a long tradition in Austria, as has speleology in general. An official expedition into Geldloch (part of the 29 km-long Ötscherhöhlensystem), a former ice-bearing cave in the Ötscher massif (Lower Austria), back in 1592 marks the first effort to explore these underground glaciers. Commanded by Reichart Freiherr von Strein on behalf of Emperor Rudolf II, the team managed to explore 860 m of cave passages and an official report was delivered to the authorities (Mais and Trimmel, 1992). Emperor Maria Theresa ordered another expedition into this cave in 1747. This time, a frozen lake stopped the explorers, but attempts were made to measure its temperature (Hartmann and Hartmann, 1984). Although these measurements were apparently flawed, the expedition leader,

Joseph Anton Nagel (later appointed mathematician at the imperial court) correctly concluded that ice formation occurs as a result of cooling of the cave during winter (Saar and Pirker, 1979). During the last few years Geldloch has become ice-free in autumn.

Eberhard Fugger, a high-school teacher who later became director of the Museum Carolino Augusteum in Salzburg (Jäger, 1919; Pillwein, 1919), pioneered instrumental research on ice caves in Austria and conducted multi-annual studies of cave air temperature and ice volume in Kolowrathöhle, now part of the 41 km-long Gamslöcher-Kolowrat-Salzburgerschacht-System, located in the Untersberg massif southwest of Salzburg (Fugger, 1888, 1891, 1892, 1893; Fig. 13.2). He visited this cave 35 times between 1876 and 1887 and also made systematic observations and measurements in two other ice caves in Untersberg, Großer Eiskeller, and Schellenberger Eishöhle (Klappacher and Mais, 1999), the latter now located in Germany. The two most prominent ice caves in Austria, Dachstein-Rieseneishöhle and Eisriesenwelt, were discovered in 1910 and 1912 (the latter actually 33 years earlier, but this went almost unnoticed), respectively, and immediately became focal points of research.

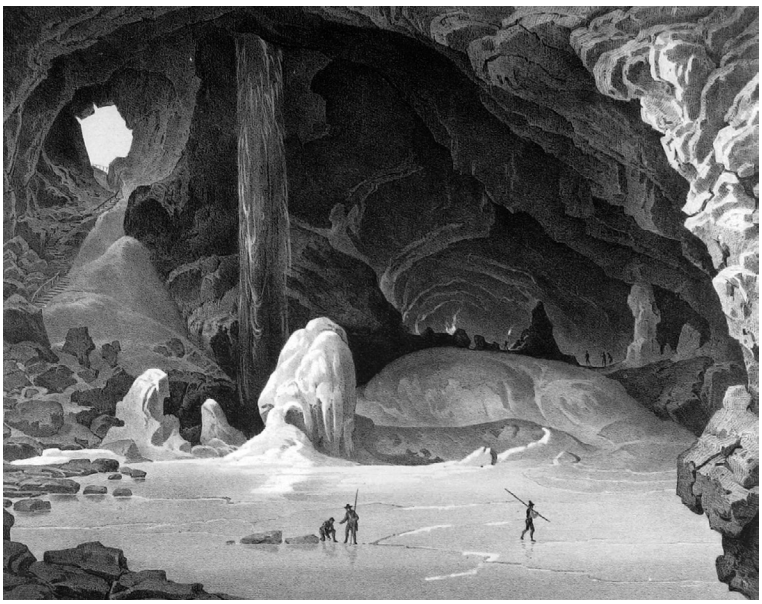

FIG. 13.2

Kolowrathöhle near Salzburg was one of the first targets of ice-cave research in the second half of the 19th century. Meanwhile this near-entrance part of the cave is largely ice-free. Copper engraving by Sebastian Stief from the middle of the 19th century.

Already in 1913, a comprehensive treatise on the physical principles of air flow and ice dynamics based on studies of caves in the Dachstein massif was published (Bock et al., 1913). Hauser and Oedl (1926) pioneered ice-cave research in Eisriesenwelt, which was the target of a dedicated expedition sponsored by the Austrian Academy of Sciences in 1921. Scientific studies in Dachstein-Rieseneishöhle were led by Kyrle and later by Saar, who conducted long-term changes in air and rock temperature, relative humidity and air flow speed and direction (Saar, 1955, 1956). Kral was the first to

conduct systematic studies of pollen in ice from alpine caves and drew conclusions about the approximate age of these ice bodies (Kral, 1968; Schmeidl and Kral, 1969).

Research since the 1980s has focused on monitoring ice-volume changes in selected ice caves (e.g., Pavuza and Mais, 1999), assessing the 3D geometry of ice bodies using ground-penetrating radar (e.g., Hausmann and Behm, 2011), and attempts to constrain the age of ice by radiocarbon-dating of enclosed organic remains (e.g., Achleitner, 1995; Mais and Pavuza, 2000; Herrmann et al., 2010). Recent years have seen a concerted effort to study the meteorology and ice dynamics of Eisriesenwelt (see below), which included the first ice core drilling performed in an alpine cave (2007), and the study of cryogenic cave carbonates (CCC), both in previously glaciated parts (Spötl and Cheng, 2014; Pavuza and Spötl, 2017) and locally also within still-existing ice bodies (Spötl, 2008).

13.3 TYPES OF ICE CAVES IN AUSTRIA

Based on their geometry and the resulting seasonal air-flow pattern, ice caves in Austria range from sag-type caves lacking a lower entrance to caves with at least two entrances at different elevations that are large enough to allow significant air flow. While these geometries give rise to distinct modes of air exchange between the cave and the outside atmosphere—traditionally (albeit not fully correctly) referred to as static vs. dynamically ventilated ice caves—combinations of the two end members are common as well, in particular in large and complexly structured cave systems, such as Schönberg-Höhlensystem (see below). It is also well known that some ice caves undergo a change from one to the other type due to opening and closing of ice plugs (e.g., Großer Eiskeller in Untersberg or Eiskogelhöhle in Tennengebirge). Such cycles have not been studied in detail, but available observations suggest that they occur on timescales of 5–10 or more years in large Austrian ice caves (Klappacher, 1996; see below).

The majority of ice caves in Austria belong to the sag type and constitute pits of less than a few tenths of meters in depth, widespread on karst plateaus of the NCA. These caves are in general smaller than those showing dynamic ventilation and a significant proportion of their ice bodies formed by transformation of winter snow that fell into these subsurface cavities. The large underground glaciers, on the other hand, mostly developed in subhorizontally oriented caves characterized by multiple entrances and a resulting intensive and seasonally changing air-flow pattern.

13.4 DISTRIBUTION OF ICE CAVES IN AUSTRIA

Ice caves are unevenly distributed across the country and occur in the following karst regions (of decreasing abundance—Fig. 13.3):

- NCA: This tectonic unit stretches from Vorarlberg, the westernmost part of Austria, to the margin of the Vienna Basin in the east, shows the highest abundance and density of karst features and host 79% of the caves in Austria. All large ice caves of this country (and the largest of the entire Alps and possibly globally) can be found in the NCA, including Eisriesenwelt, Dachstein-Rieseneishöhle, Eiskogelhöhle, Schwarzmooskogel-Eishöhle and ice-bearing parts within the giant Schönberg-Höhlensystem (see below). Also, the largest ice bodies of sag-type caves can be found here, such as Kraterschacht in Sengsengebirge, which hosts a snow-firn-ice body of some 70 m in thickness (Weißmair, 1995, 2011), and Hochschneid-Eishöhle in Höllengebirge,

which was recently explored and contains a firn and ice plug of about 70 m thickness. The NCA also host the lowest-elevation ice cave in this country, Schödlkogeleishöhle near Bad Mitterndorf (Styria), located at 939 m a.s.l., which is currently at the verge of transforming into a seasonal ice cave. Fig. 13.3 shows that within the NCA ice caves are particularly abundant between Salzburg and Styria, which reflects the presence of large karst plateaus in this region reaching up above the timberline (located between about 1600 and 1800 m a.s.l. in the NCA), with elevation ranging from about 1500 to almost 3000 m a.s.l.

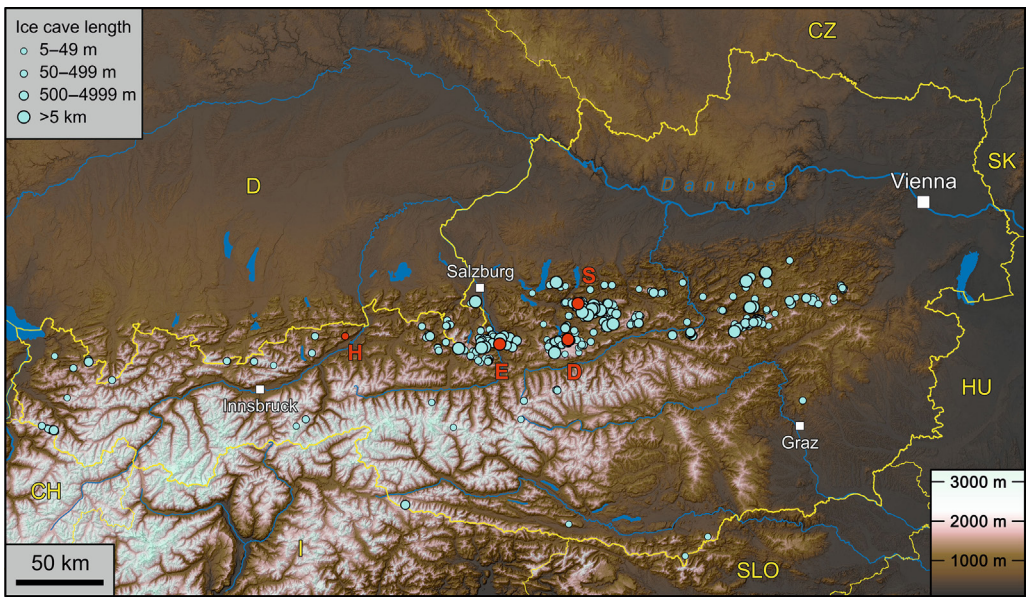

FIG. 13.3

Elevation map of Austria showing the distribution of ice caves differentiated according to their length. Note that the latter figure refers to the total length of the cave, not the length of the ice-bearing part. H, Hundsalm Eis- und Tropfsteinhöhle; E, Eisriesenwelt; D, Dachstein-Mammuthöhle; S, Schönberg-Höhlensystem.

- Central Alps: They form the main ridge of the Eastern Alps, include the highest summits, are partly glaciated and consist of metamorphic rocks. Although caves are known there up to about 2900 m a.s.l., most of these high-alpine caves are less than a few hundred (and often less than a few tens of) meters in length and no large ice bodies are known there. The scarcity of ice caves in the highest mountain ranges of the Eastern Alps may appear surprising, but is primarily due to the predominance of non-karstic silicate rocks.
- Southern Calcareous Alps: This narrow band of both non-metamorphic and low-grade metamorphic carbonate rocks straddles along the southern border of Austria. Karst abounds only in some regions, such as in the eastern Karawanken Mountains, and only few ice-bearing caves are known, most notably Obstanser Eishöhle. This cave opens at 2192 m a.s.l. near the western end of the Karnischer Hauptkamm, comprises 3.4 km of passages and contains some perennial ice behind its main entrance (Herrmann, 2017). Back in 1934, the then-known cave parts were

precisely surveyed using professional geodetic instruments (Killian, 1935). This dataset provides clear evidence that the ice volume has decreased since then, with an apparent acceleration since the early 1980s. Instrumental monitoring since 2008 has revealed a near-linear lowering of the ice height at two locations (Spötl et al., 2017). Based on this trend, Obstanser Eishöhle will likely completely loose its perennial ice in the near future.

The nationwide database on Austrian ice caves allows the exploration of the factors controlling their occurrence. The fact that ice caves are known to be present across an altitudinal range of 2 km clearly shows that elevation (and hence atmospheric temperature) is not the main controlling factor. Fig. 13.4 reveals that the highest abundance of ice caves occurs between about 1800 m and 2100 m a.s.l., which is well below the elevation of the 0°C annual isotherm of the atmosphere in the Alps (based on long-term measurements at meteorological stations).

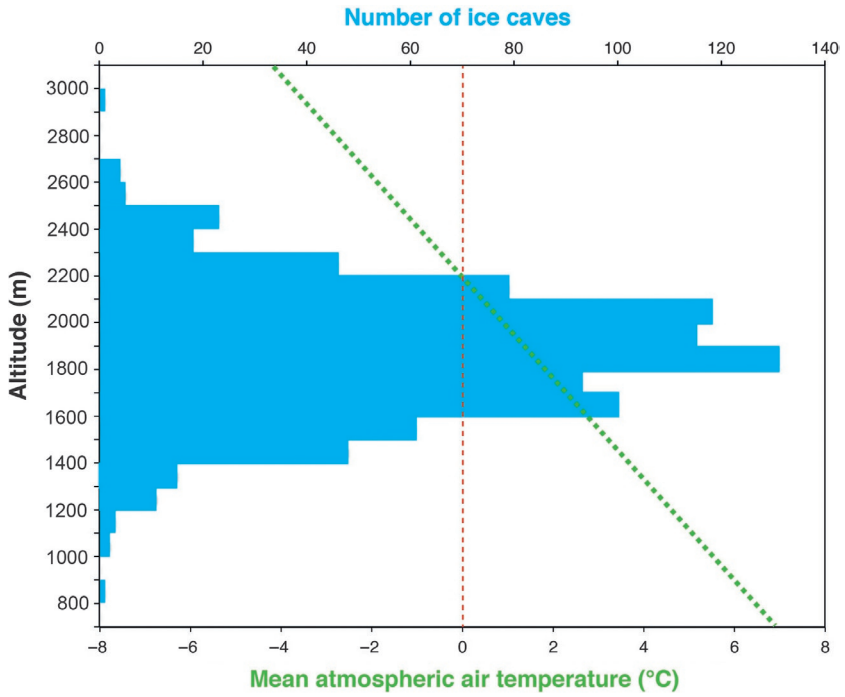

FIG. 13.4

Altitudinal distribution of ice-bearing caves in Austria. The *green dotted line* is the mean annual air temperature in the Eastern Alps and the *red dotted line* marks 0°C.

Ice caves are thus unrelated to Alpine permafrost, whose lower boundary is presently located at about 2500 m in the Central Alps. The altitudinal distribution of ice caves instead largely reflects a combination of the abundance of (uplifted) cave systems between about 1500 m and 2000 m a.s.l. and the decreasing likelihood of preserving cave ice at elevations below about 1400 m a.s.l.

The average lapse rate in the Eastern Alps is about 0.5°C/100 m, and the interior air temperature of most caves follows this trend. Ice-bearing cave parts are notable exceptions showing deviations of up to 4°C towards lower temperatures (Fig. 13.5).

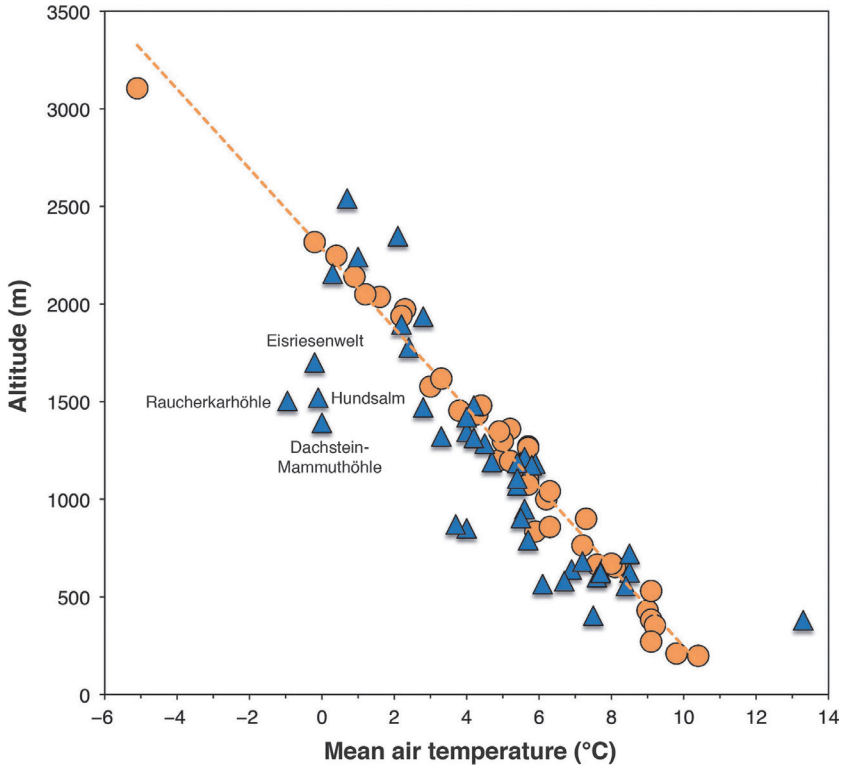

FIG. 13.5

The interior temperature of Austrian caves *(blue triangles)* corresponds approximately to the long-term average of the outside atmosphere *(orange dots)* at a given altitude. The overall cave air gradient follows that of the atmosphere (*orange line* based on data from selected climate stations in Austria; period 1981–2010). Ice-bearing cave (parts) deviate significantly from this altitude trend and four are labeled: the ice-bearing frontal part of Eisriesenwelt, the upper ice-bearing level of Hundsalm Eis- und Tropfsteinhöhle, Raucherkarhöhle (*Eisstadion*) as part of Schönberg-Höhlensystem, and the ice-bearing part of Dachstein-Mammuthöhle close to its western entrance.

Seven of Austria's 30 show caves contain perennial ice. These include the three large ice caves Eisriesenwelt, Dachstein-Rieseneishöhle and Eiskogelhöhle, as well as the small ice caves Prax-Eishöhle and Hundsalm Eis- und Tropfsteinhöhle as well as a small part of Frauenmauer-Langstein-Höhlensystem. Parts of Dachstein-Mammuthöhle aside the touristic route also contains some cave ice (see below).

Touristic use of ice caves in Austria started in 1845 in Kolowrathöhle near Salzburg. Guided tours into the two best known caves, Dachstein-Rieseneishöhle and Eisriesenwelt, commenced in 1912 and 1920, respectively. The former was already illuminated by electrical lights in 1928. In recent years, the

Austrian ice caves have been visited by a few hundred thousand guests per year, providing important local touristic and economic incentives.

In addition to ice caves, Austria hosts a few touristic, partly artificial, glacier caves, which—given the strong retreat of alpine glaciers—commonly exist only for a few years. An exception is Natur Eis Palast, an artificially modified glacier cave at 3200 m a.s.l., which provides insights into the geometry and morphology of open fractures in the uppermost part of Hintertux Glacier (Zillertal Alps).

13.5 EXAMPLES OF ICE CAVES IN AUSTRIA

In this chapter four ice caves are briefly presented, which are among the best studied in Austria.

13.5.1 EISRIESENWELT

As the name suggests this cave south of Salzburg hosts a tremendous ice body, which ranks among the largest cave ice accumulations worldwide. Eisriesenwelt opens on the western flank of Tennengebirge at 1657 m a.s.l., about 1150 m above the level of the adjacent Salzach Valley (47.511°N, 13.193°E). The cave comprises at least 42 km of predominantly horizontal passages (Pointner and Klappacher, 2016), which belong to a Miocene-age paleophreatic cave level.

The first approximately 1 km of this cave system contains perennial ice, reaching a thickness of up to several meters (Fig. 13.6) and comprising a surface area of 28,000 m^2. The ice starts right behind the entrance and consists of floor ice, a few several meter-tall stalagmites, stalactites and seasonal hoar frost.

FIG. 13.6

Layered ice containing fine crystalline cryogenic calcite particles exposed in the interior of the glaciated part of Eisriesenwelt.

Photo courtesy of Robbie Shone.

Eisriesenwelt shows a bidirectional air-flow pattern typical of dynamically ventilated caves. During the warm season, the draft at the otherwise-closed entrance gate reaches 13 m/s, while during winter cold outside air is drawn into the cave, warms upon contact with the rock walls and ascends through unexplored chimneys toward the plateau 400–500 m higher. During winter, the 0°C isotherm progressively moves further into the cave, and seasonal ice formations are locally present several hundred meters behind the main ice-bearing part. Detailed measurements show, however, that this simple air-flow pattern is often perturbed (Thaler, 2008; Obleitner and Spötl, 2011; Schöner et al., 2011). Temperatures at different depths in a 7-m-deep hole at *Eispalast* mirror these seasonal and shorter-term air temperatures changes with a slight delay, as do radon measurements, being particularly sensitive to ventilation changes of cave air (Gruber et al., 2014). The temperature at the base of the ice body at *Eispalast* varies between −0.1 and −0.5°C (Fig. 13.7), i.e., the ice is permanently frozen to bedrock (or gravel or loam covering bedrock).

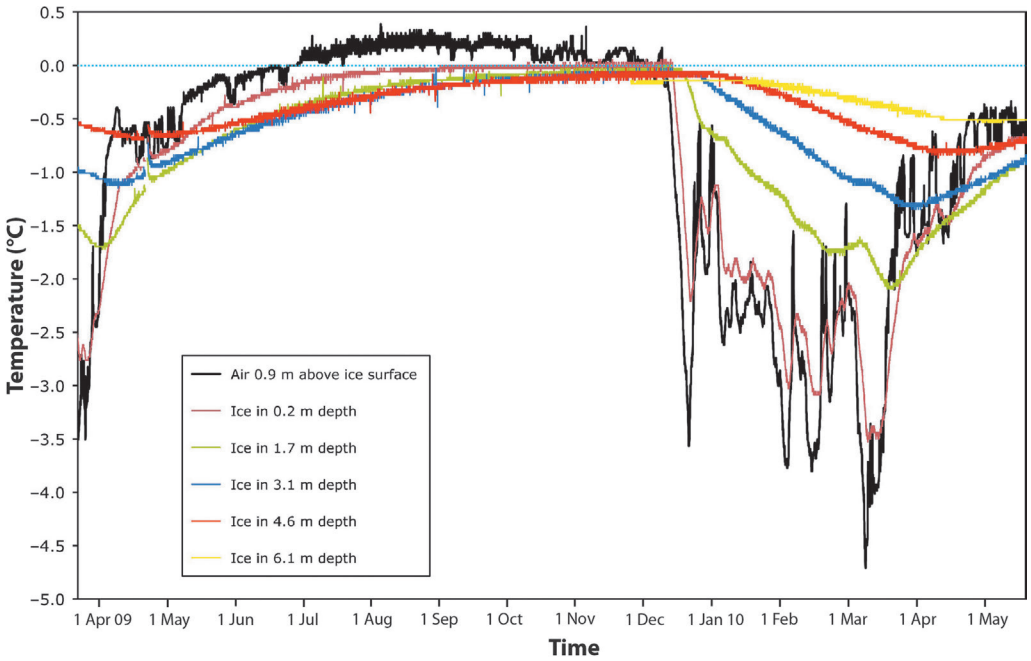

FIG. 13.7

Temperature distribution at different depths in the ice body at *Eispalast* near the inner limit of the glaciated part of Eisriesenwelt (about 500 m behind the entrance) over the course of about 1 year. Note delayed response of the ice temperature to seasonal cooling by cold winter air being drawn into the cave.

Since 1920, when this cave was developed as a touristic cave, the summer air flow out of the cave has been restricted by a door. This door remains open during the cold season allowing the cold winter air to freely enter the cave. Due to these artificial measures, the climate of this cave and hence its ice mass balance have been modified, in particular during summer and autumn. Only scattered reports exist about decadal-scale ice-volume changes (e.g., Abel, 1965; Gressel, 1965) and these in conjunction with photographic documents indicate that, e.g., a side passage called *Wimur*, leading to a second lower

entrance at 1838 m a.s.l. also acts as a lower opening of the cave ventilation system. It was glaciated during the first half of the 20th century and became ice-free since then. A narrow restriction leading to *Eispalast* deeper into the cave (*Eistor*) has been progressively widened by ice ablation since the 1920s.

More recently, the ice cave was surveyed using terrestrial laser-scan techniques, providing an accurate and precise figure of the glaciated area (28,000 m^2) and a reference for future long-term mass balance monitoring (Petters et al., 2011; Milius and Petters, 2012).

In a large chamber called *Eispalast* at the inner end of the ice-bearing part, measurements using ground-penetrating radar (and verified using steam drilling) revealed an ice thickness between 1.5 and 7.5 m (Behm and Hausmann, 2007; Hausmann and Behm, 2011). There, an ice core was drilled to bedrock in June 2007, the first ice-core drilling ever performed in an alpine ice cave. Tritium analyses showed that ablation has led to an almost complete loss of bomb-derived tritium removing any ice accumulated since at least the early 1950s. Attempts to constrain the age of the 7.1 m-long ice profile were largely unsuccessful given the high purity of this ice. A crude estimate based on radiocarbon dating of particulate organic matter suggests a basal ice age in the order of several thousand years (May et al., 2011).

An earlier study by Fritz (1977) examined four samples of Eisriesenwelt (from *Großer Eisdom* near the entrance and from *Mörkgletscher* near the inner end of the ice-bearing cave part) and found low pollen concentrations and pollen spectra that included pollen of cultivated plants. The author concluded that these ice samples are likely less than a few hundred years old.

The ice of Eisriesenwelt commonly contains cryogenic cave carbonates (CCC), whose crystal size typically ranges from about 0.1 to 0.4 mm. At the ice cliff of *Mörkgletscher* several distinct layers of these carbonate particles are exposed (Spötl, 2008; Fig. 13.6), but attempts to date them using U-Th were unsuccessful. Cryogenic carbonates were also frequently encountered in the drill core in *Eispalast* (May et al., 2011). No coarse crystalline varieties of CCC were found in the ice-bearing part of this cave, reflecting its dynamic meteorology. Coarse crystalline CCC, however, was found in a remote and currently ice-free part of the Eisriesenwelt and yielded a late glacial age (C. Spötl and M. Luetscher, unpublished data).

13.5.2 SCHÖNBERG-HÖHLENSYSTEM

Located in the western part of Totes Gebirge, Austria's most extensive karst plateau, this giant cave system has 34 entrances between 1459 m and 1933 m a.s.l. and encompasses 146.7 km of passages and 1061 m of vertical extent (47.718°N, 13.787°E; Geyer et al., 2016). It is the result of a successful merger between Raucherkarhöhle (Zeitlhofer and Knobloch, 2008) and Feuertal-Höhlensystem (Jansky et al., 2008) in 2007. The complex geometry in combination with the multiple entrances gives rise to a dynamic ventilation pattern. While the general air flow direction in summer is from the high-lying Feuertal-Höhlensystem towards the lower lying Raucherkarhöhle (Fig. 13.8) and vice versa in winter, there are a variety of local complexities including areas of stagnant air.

The majority of Schönberg-Höhlensystem is ice-free. Perennial ice accumulations are only found near the entrances of Feuertal-Eishöhle (part of the Feuertal-Höhlensystem; *Gustave-Abel-Halle*), Raucherkarhöhle (*Eingangslabyrinth*) and Altarkögerlhöhle. The first two are well documented and are briefly presented here.

Feuertal-Eishöhle opens at 1718 m a.s.l. near the base of a large doline occupied by a steep snowfield, which does not completely disappear in late summer. This snowfield shows the transition into firn

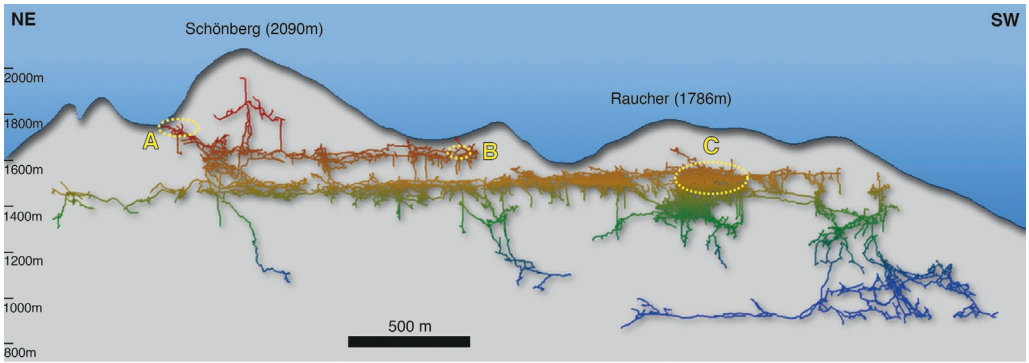

FIG. 13.8

Vertical section of Schönberg-Höhlensystem showing the location of the three ice-bearing parts. (A) Ice part of Feuertal-Eishöhle, (B) ice part of Altarkögerlhöhle, (C) ice part of Raucherkarhöhle. The depth distribution of this giant cave system is color-coded. Based on survey map by Harald Zeitlhofer.

in its deeper part and extends into the ice-bearing entrance hall of the cave. This 60×40 m wide hall also receives snow via two shafts reaching to the surface forming prominent snow cones. Photographs document that the ice level in this near-entrance hall did not change significantly over several decades (Fig. 13.9). This is confirmed by regular surveys of the ice height along traverses which show no trend since 1999 (Fig. 13.10).

FIG. 13.9

View from the ice floor in Feuertal-Eishöhle towards the snow cone of the doline in the background. The ice cover in this hall was roughly at the same level in 2016 (right) as in 1931 (left).

Right photo courtesy of Harald Zeitlhofer.

Meltwater that does not refreeze in the entrance hall finds its way via a narrow and strongly ventilated connection (*Bläser*, also referred to as *Eisbläser*) and a steep glaciated ramp into *Gustave-Abel-Halle*. In the past, this connection was repeatedly clogged by ice for several years disconnecting Feuertal-Eishöhle from the rest of Schönberg-Höhlensystem. During these episodes, the entrance hall was commonly occupied by a shallow ice lake. The ramp terminates with a prominent ca. 10 m-high ice wall towards *Gustave-Abel-Halle*. Photographs and survey data show that the volume and dimensions

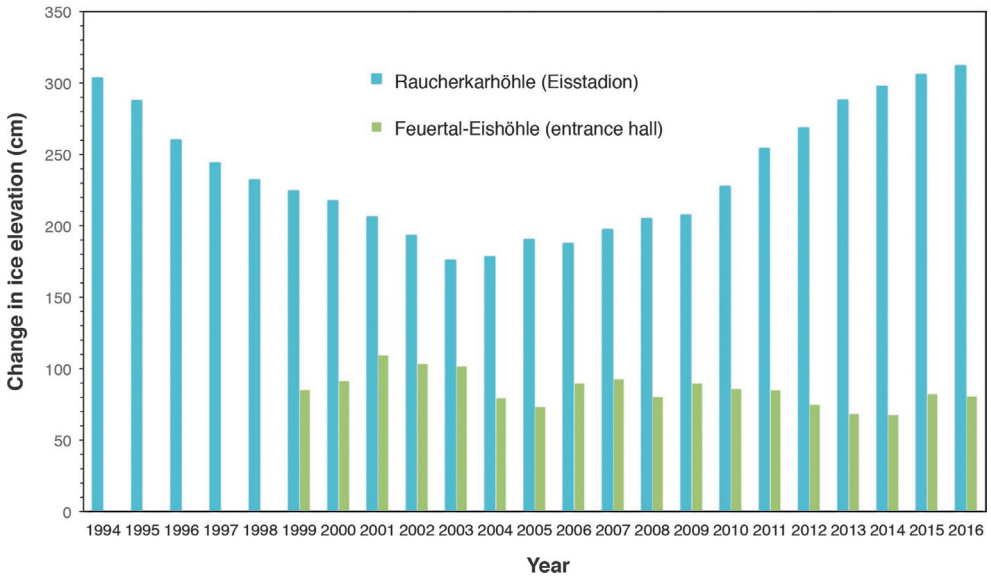

FIG. 13.10

Long-term evolution of ice height (approximately corresponding to ice thickness) in Feuertal-Eishöhle and Raucherkarhöhle. Each data point represents the mean of 10–11 measurements points along a traverse across the ice surface.

of this ice wall in 1928 was comparable to the situation in 2016. At the beginning of the 21st century, the cliff face retreated somewhat, exposing layered ice (Fig. 13.11).

In recent years, new ice has covered the cliff (Fig. 13.11) and the passage leading deeper into the cave was again buried by ice in 2016. Hence the ice in *Gustave-Abel-Halle* shows a cyclic behavior

FIG. 13.11

The ice wall leading into *Gustave-Abel-Halle* of Feuertal-Eishöhle c.1931 (left; Abel, 1932), 2003 (middle) and 2016 (right).

Middle and right photos courtesy of Clemens Tenreiter and Harald Zeitlhofer, respectively.

with periods lasting 1–3 decades. Historical reports show that, e.g., the *Bläser* connection was closed in 1958, open in 1980, and closed again in the 1990s. Surveys of the ice body in the entrance hall show no systematic trend since the onset of these measurements in 1999 (Fig. 13.10).

In Raucherkarhöhle, the ice-bearing parts are also found close to the entrance and initially comprised several galleries including *Planer-Eishöhle*, which later was connected to the main cave system. Already at the time of discovery (1961), most ice formations showed clear signs of degradation. During the subsequent decades, the ice disappeared from all of these cave parts and small remnants only remained in *Pfeilerhalle*, *Pilzlinghalle*, *Rauhreifgang* and *Planer-Eishöhle*. The complete deglaciation of *Kleiner Rundgang* led to the discovery of new passages including *Eisstadion*, a 25 × 35 m wide hall. At the time of discovery (1993) about two thirds of this hall were occupied by a thick, layered ice body showing a near-horizontal surface. Currently, *Eisstadion* is the largest remaining ice accumulation in Raucherkarhöhle. Regular surveys started in 1994 and reveal a gradual decline ice height over the subsequent decade (Fig. 13.10). This trend, however, reversed in 2005, and since then, this cave part has shown a net ice increase. The reason for this decadal change in ice mass balance was a change in air circulation: Prior to 1998 air temperatures at *Eisstadion* were always slightly above freezing, even during winter (Fig. 13.12). In 1998, a new connection opened in the ice between *Eisstadion* and *Pilzlinghalle* due to wind ablation and dripping water.

This narrow hole widened in the following years and allowed the inflow of cold winter air into *Eisstadion* and *Großer Eissaal* (the latter was completely ice-free at that time). Already in 1998, new ice formation was

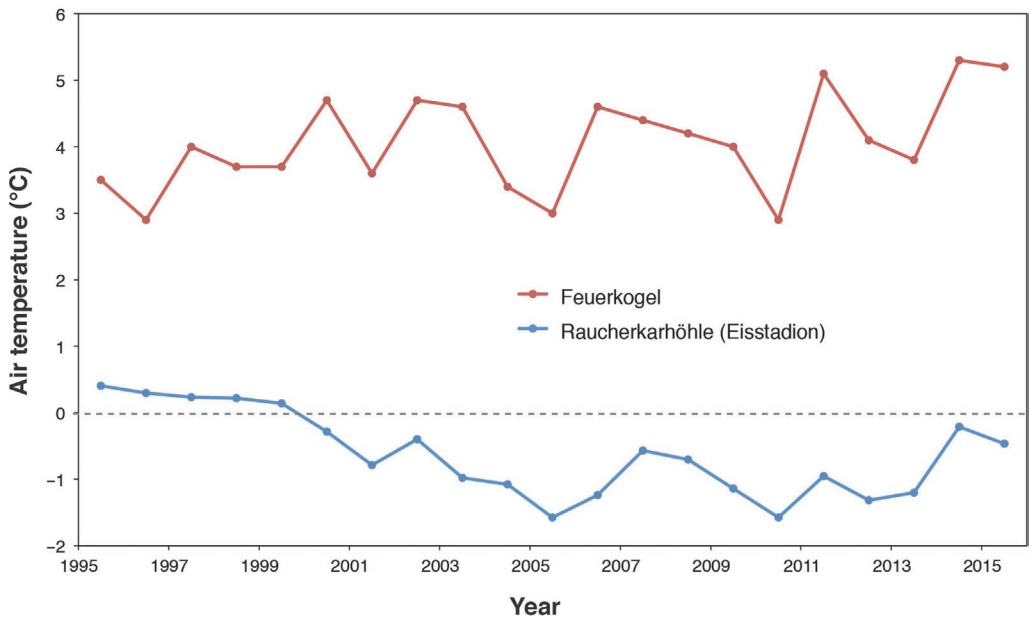

FIG. 13.12

Comparison between the decadal-scale cooling trend in the near-entrance parts of Raucherkarhöhle and the opposite trend of the outside atmosphere as recorded by the meteorological station at Feuerkogel (1618 m a.s.l.) located 13 km NNW of the cave (annual means).

observed locally. This new cycle of winter cooling terminated the decadal trend of ice decline at *Eisstadion* and initiated a new cycle of ice accumulation, albeit with a delay of several years (Fig. 13.10).

A model summarizing the complex interplay between cave air ventilation and ice mass balance was presented by Wimmer (2008). Its predictions regarding ice volume changes have been validated by observations made in the years since then. The positive ice volume trend continues. In *Großer Eissaal*, which had been ice-free for two decades, large ice columns as well as floor ice formed. A comparison of photographs demonstrates that there is already more ice in this chamber than in 1965 when it was discovered (Fig. 13.13).

FIG. 13.13

Ice formations in *Großer Eissaal* at the time of discovery (1965, left) and in 2016 (right), soon after a new cycle of ice accumulation had commenced. In between, this cave chamber had been continuously deglaciated for 20 years.

Left photo courtesy of Helmuth Planer.

It is expected that this positive ice mass balance trend in *Eisstadion* and *Großer Eissaal* will continue for many years, possibly decades. This cyclic behavior appears to be only marginally influenced by the general warming trend in the Alps. On the other hand, other parts of Raucherkarhöhle are more vulnerable to climate warming, e.g., *Planer-Eishöhle*. This cave part shows an uninterrupted ice retreat since many years, reflecting its near-surface setting and insufficient winter cooling.

13.5.3 DACHSTEIN-MAMMUTHÖHLE

The Dachstein is situated in the central part of the NCA and comprises a major uplifted karst region 580 km^2 in size. It southern side reaches up to almost 3000 m a.s.l. and is partly glaciated. On the northern rim, the plateau shows a prominent escarpment towards Hallstätter See, a deep lake of glacial origin at 508 m a.s.l. Along this escarpment several large caves are known, which include from west to east Hirlatzhöhle (104.8 km long), Dachstein-Mammuthöhle (67.4 km), Mörkhöhle (4.2 km), Dachstein-Rieseneishöhle (2.7 km) and Schönberghöhle (9.3 km). High-discharge karst springs are located below the levels of these paleophreatic cave systems.

Dachstein-Mammuthöhle is currently the fourth longest cave in Austria with a vertical extension of 1.2 km (47.534°N, 13.708°E). The system is labyrinthic and comprises 21 entrances between 927 and 1828 m a.s.l. (Behm et al., 2016). Most paleo(epi)phreatic passages are located between 1250 m and 1550 m a.s.l. and show a long and complex speleogenetic history (e.g., Plan and Xaver, 2010).

Perennial cave ice is present near the western entrance (*Westeingang*), which opens at 1391 m a.s.l. Since the 1990s, this ice as well as that of the nearby Dachstein-Rieseneishöhle have been targets of

annual ice level measurements in combination with cave air monitoring (Mais and Pavuza, 1999, 2000). In contrast to Dachstein-Rieseneishöhle, whose cave meteorology and hence ice volume and distribution are significantly modified by the show cave management, the ice in Dachstein-Mammuthöhle is fairly undisturbed. Ice is present in two places not far from the western entrance, *Feenpalast* and *Saarhalle*, located some 100–150 m apart from each other but well separated from the touristic parts of the cave with respect to the ventilation regime. In the 1970s and 1980s the thickness of this horizontally layered ice still reached a thickness of up to 15 m. Georadar measurements conducted in 2007 revealed a thickness of the ice bodies at *Feenpalast* and *Saarhalle* of only up to 9 and 6 m, respectively (Behm and Hausmann, 2007; Hausmann and Behm, 2011). Prominent reflectors in the radar data appear to be related to layers rich in fine-crystalline cryogenic carbonate particles which, however, have not yet been sampled and analyzed. A constant decline of 30–40 cm/year was observed in *Feenpalast* since the onset of systematic level measurements in the 1990s (Spötl and Pavuza, 2016, Fig. 13.14).

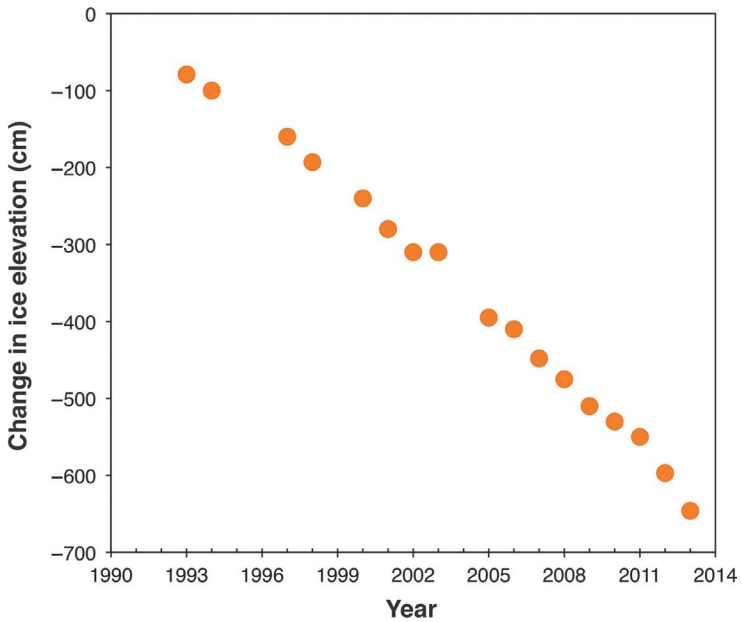

FIG. 13.14

Gradual decline of the ice height as monitored in *Feenpalast* of Dachstein-Mammuthöhle.

As there is also a significant lateral retreat of the ice body, the degradation of the ice is actually accelerating. If this trend persists the upper part of *Feenpalast* will be ice-free within the next 5 years.

A significantly slower but also almost linear decline of the ice of about 7–8 cm/year was observed in *Saarhalle* since the 1990s.

Organic material recovered close to the base of the ice at the retreating cliff in the highest part of *Feenpalast* yielded a radiocarbon age of 695 ± 35 BP (Mais and Pavuza, 2000; 1260–1389 cal AD, 2 sigma range) indicating that at least this part of *Feenpalast* was free of ice prior to the Little Ice Age. Two wood samples from deeper layers are slightly older (Table 13.1).

Fig. 13.15 shows a series of images taken at the ice cliff in *Feenpalast*, documenting the lowering of ice surface over the last two decades and the appearance of a prominent hole.

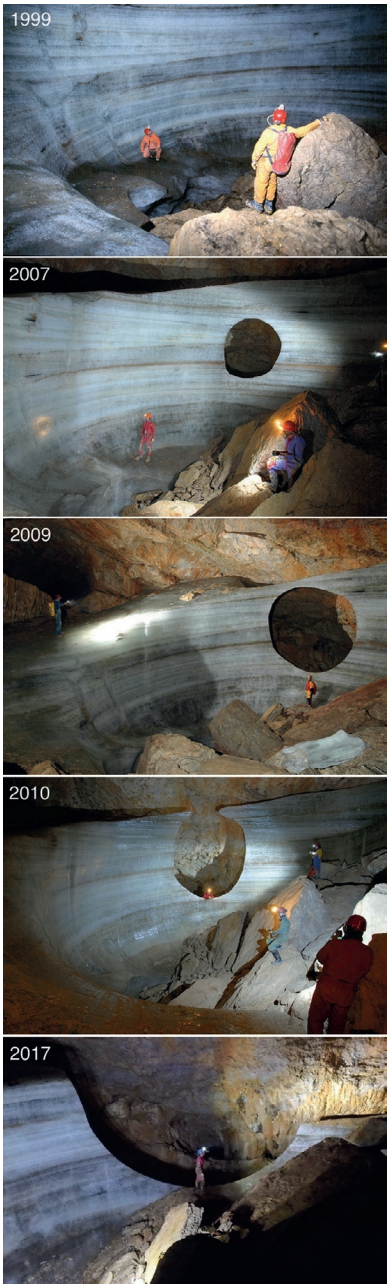

FIG. 13.15

Retreat of the ice body in *Feenpalast* over the course of 18 years. A small gallery with air flow led to the formation of the hole in the thin ice rim.

Photos from 1999, 2007, and 2010 courtesy of Heiner Thaler.

In September, 2009, a 5.3 m-long ice core was drilled at the site in *Saarhalle* showing the greatest ice thickness. During drilling, small amounts of liquid water were extracted at depths between 3.3 and 3.6 m. No melting of the ice, however, was observed at the base of the ice body. Tritium analyses of core samples indicate more than one source of water of different origin and age. The upper 1.2 m of ice most likely originated from precipitation fallen before the 1960s (based on Tritium data; Kern et al., 2011), i.e., younger ice layers have been lost by ablation similar to the situation at *Eispalast* of Eisriesenwelt (see above).

In nearby Dachstein-Rieseneishöhle there is some evidence that the ice level at the turn of the millennium was comparable to that during the 1930s, as documented by postcards (Mais and Pavuza, 1999). Unfortunately, such data are not available for the ice-bearing galleries of Dachstein-Mammuthöhle.

13.5.4 HUNDSALM EIS- UND TROPFSTEINHÖHLE

Located north of Wörgl in the lower Inn Valley of Tyrol (47.545°N, 12.027°E), this cave is an example of the many small sag-type caves in the NCA which contain perennial ice accumulations due to trapping of cold winter air. Hundsalm Eis- und Tropfsteinhöhle, however, is the only touristic ice cave in western Austria (which opened in 1967) and also the westernmost ice show cave in the western part of the Alps. The cave developed along a steeply dipping fault and has two adjacent shaft-type entrances, one higher than the other by a few meters. The lower of these two pits opens at 1520 m a.s.l. and is used to enter the cave via a staircase. The two shafts are crucial for the cooling of the cave during winter. Monitoring has shown that due to its slightly greater height (25 m) and larger diameter, the upper entrance acts as a "chimney" in winter, allowing cave air to ascend and exit the cave because of its lower density than the outside winter air. As a consequence, cold and dense outside air is drawn into the cave via the lower entrance (whose gated entrance is kept open during winter). This cold air cools the cave walls (Fig. 13.16) and the ice body and also results in a drying of the cave. While Hundsalm Eis- und Tropfsteinhöhle shows a dynamic air exchange at times when the outside air temperature drops below about −2°C, it acts as a "cold air trap" during the rest of the year with air cave air temperatures within a few tenths of a degree of the freezing point in the ice-bearing part and temperatures between 1.5 and 2.0°C in the southern, ice-free part.

Ice forms in two ways in this cave, as congelation ice and via transformation of snow and firn. The former results in the formation of seasonal ice stalagmites, stalactites and ice covering walls, but contributes only locally to the formation of floor ice. Snow enters the cave via both shafts and firn and grainy ice resulting from firn recrystallization constitutes a major part of the several meter-thick deposits in the northern part of the cave. Since 1967, when this cave was developed as a show cave, the snow and ice mass balance has been manipulated, because snow has been artificially introduced into the cave during mid-winter (in an attempt to preserve the ice body). In addition, the entrance shaft was slightly widened (and gated). Despite these measures, recent years have shown (a) an uninterrupted decline in the elevation of the main ice body (about 0.9 m since 2007), (b) a widening of the gap between the ice body and the cave wall (reaching 0.5–1 m), (c) generally less seasonal ice, and (d) a shorter "survival time" of these seasonal ice formations (disappearing in late summer). These observations in conjunction with long-term temperature data suggest that the cave will likely lose its perennial firn and ice deposits in the not too distant future, largely due to warmer and drier winters, which provide insufficient cooling of the cave to "survive" the warm season. A similar trend has been observed in other small ice

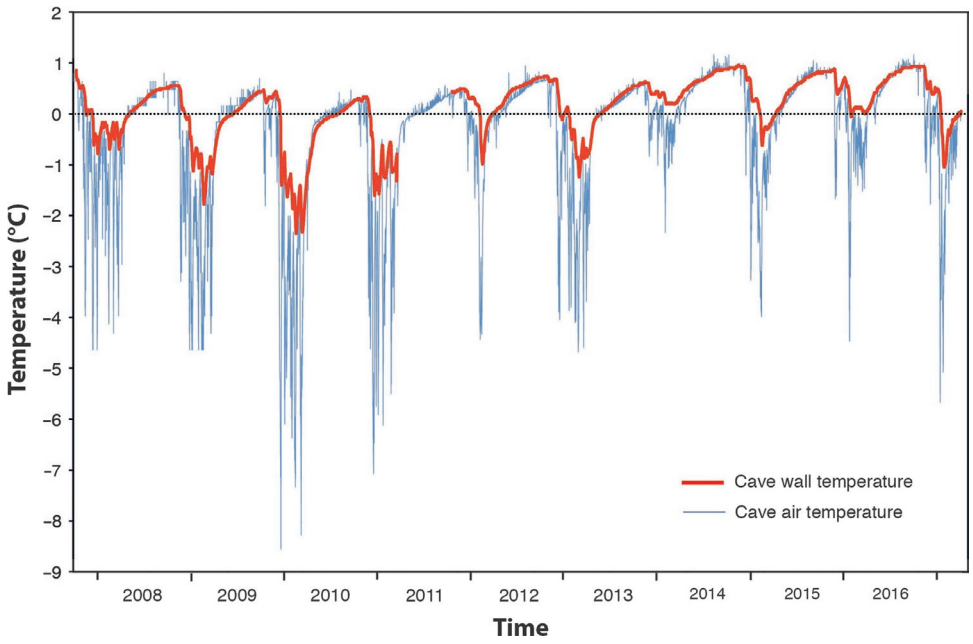

FIG. 13.16

During the last decade both the number of days with negative temperatures and the magnitude of winter cooling of the wall rock at Hundsalm Eis- und Tropfsteinhöhle as measured in a borehole at 1.3 m depth have decreased. The extent of seasonal winter cooling of the rock surrounding the cave is a function of the cave air temperature (measured in the same chamber).

caves in Austria (Spötl and Pavuza, 2016), including Prax Eishöhle in Loferer Steinberge, which has transformed into a seasonal ice cave in the past few years.

Historical documents show that Hundsalm Eis- und Tropfsteinhöhle contained much more ice when discovered in 1921 (Spötl, 2013), a time when alpine glaciers were also advancing. Radiocarbon dating of 19 wood fragments embedded in the deeper part of the up to 7 m thick firn and ice body provide clues about the long-term history (Spötl et al., 2014). This is the largest radiocarbon dataset for an Alpine ice cave and a summary of all dated samples currently available from ice caves in Austria is provided in Table 13.1. Although some of these fragments from Hundsalm Eis- und Tropfsteinhöhle may have been reworked during previous ablation episodes, the frequency distribution shows a clear maximum between the 15th and the 17th century (with samples dating back to the 13th century AD; Fig. 13.17), which coincides with the coldest centuries of the Little Ice Age, when East Alpine glaciers reached their Holocene maxima (Holzhauser et al., 2005; Nicolussi and Patzelt, 2000). An earlier period of ice build-up is dated to the 6th and 7th centuries AD, also coinciding with a cool climate (Büntgen et al., 2011) and positive glacier mass balances in the Alps. No samples date back to the first half of the Holocene. This is also confirmed by studies from other ice caves in Austria and the oldest dated wood samples are from the early part of the 5th millennium AD (Eisgruben-Eishöhle, Sarstein and Schneeloch, Schneealpe—Achleitner, 1995; Herrmann et al., 2010). This lack of wood fragments may be regarded as a hint that at least some Alpine ice caves were probably ice-free during most of the first

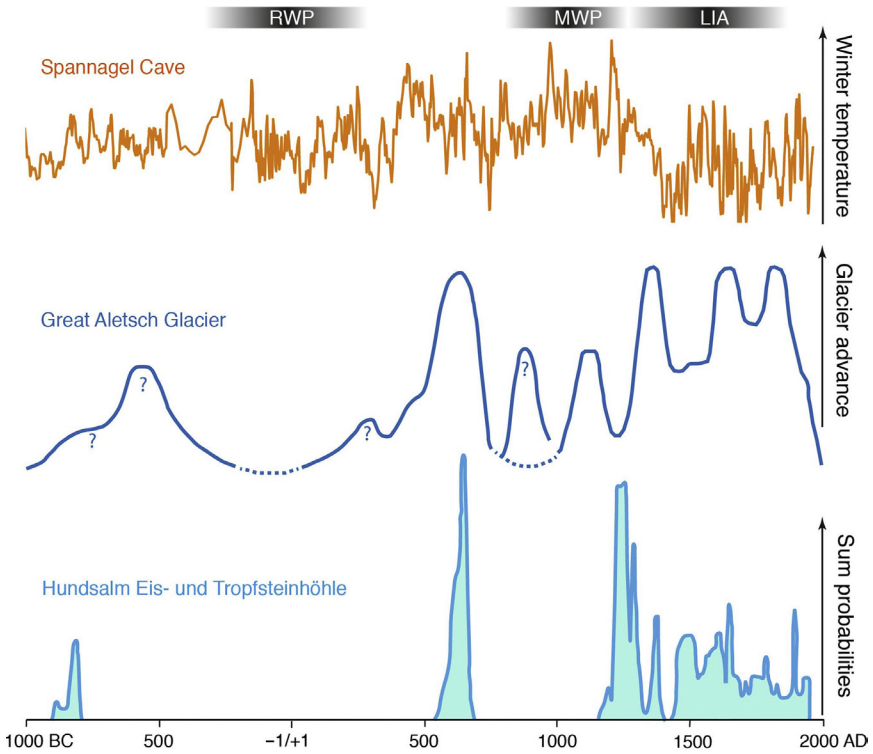

FIG. 13.17

Comparison between the abundance of radiocarbon-dated wood remains retrieved from the ice of Hundsalm Eis- und Tropfsteinhöhle (Spötl et al., 2014), length changes of Great Aletsch Glacier in Switzerland (Holzhauser et al., 2005) and winter temperatures reconstructed from oxygen isotopes in stalagmites from Spannagel Cave in western Austria (Mangini et al., 2005; Fohlmeister et al., 2013) over the past three millennia. RWP, Roman Warm Period; MWP, Medieval Warm Period; LIA, Little Ice Age.

half of the Holocene—a time interval characterized by generally negative mass balances also of Alpine glaciers (e.g., Joerin et al., 2008; Ivy-Ochs et al., 2009).

A microbiological study examined ice samples from the deep part of this ice body and found abundant bacteria (actinobacteria; Sattler et al., 2013). Cyanobacteria were also identified and were likely introduced from outside. Overall, the microbial community resembled communities known from accumulations of organic and inorganic material on Alpine glaciers (known as cryoconite).

As the name suggests, Hundsalm Eis- und Tropfsteinhöhle hosts both ice and speleothems, a combination which is rather uncommon. Studies have shown, however, that the speleothems in the ice-bearing part are ancient. The cave also contains a lower level, and the narrow connection between the two cave parts, which was artificially opened to allow exploration in 1984, was later closed by a door to prevent air exchange. This lower cave level has a temperature of 4.2 ± 0.1°C, no ice, but active speleothem deposition, including abundant moonmilk (Reitschuler et al., 2012, 2015).

Table 13.1 Summary of Radiocarbon Dates of Organic Remains in East Alpine Ice Caves

Cave (Mountain Range)	Elevation of Main Entrance (m a.s.l.)	Lab Code	Conventional ^{14}C Age BP	Calibrated ^{14}C Age (2 Sigma)[a]	Reference
Eisgruben-Eishöhle (Sarstein)	1720				
		74,817	2210 ± 70	400–91 BC (0.99) 67–65 BC (0.01)	Achleitner (1995)
		74,818	4520 ± 50	3366–3088 BC (0.97) 3058–3030 BC (0.03)	Achleitner (1995)
Schneeloch (Schneealpe)	1450				
		LTL3900A[b]	2228 ± 50	395–184 BC (1.00)	Herrmann et al. (2010)
		LTL4709A[b]	242 ± 45	1495–1507 AD (0.01) 1511–1601 AD (0.21) 1616–1689 AD (0.39) 1729–1810 AD (0.31) 1925–1950[c] (0.08)	Herrmann et al. (2010)
		GrN-32288	4360 ± 30	3085–3064 BC (0.06) 3028–2904 BC (0.94)	Herrmann et al. (2010)
Beilstein Eishöhle (Hochschwab)	1308				
		GX-33495	700 ± 65	1216–1404 AD	Pavuza (unpubl.)
		GX-33634	200 ± 100	1495–1601 AD (0.15) 1616–1950[c] (0.85)	Pavuza (unpubl.)
		GrA-29972	135 ± 30	1672–1778 AD (0.43) 1799–1892 AD (0.41) 1907–1942 AD (0.16)	Pavuza (unpubl.)
Dachstein-Mammuthöhle (Dachstein)	1391				
			695 ± 35	1260–1316 AD (0.73) 1354–1389 AD (0.27)	Mais and Pavuza (1999), Kern et al. (2011)
			751 ± 45	1188–1300 AD (0.98) 1368–1381 AD (0.02)	Plan and Pavuza (unpubl.)
			1133 ± 40	776–794 AD (0.06) 799–988 AD (0.94)	Plan and Pavuza (unpubl.)
Kraterschacht (Sengsengebirge)	1531				
		LTL4510A	886 ± 45	1032–1224 AD (0.98) 1234–1242 AD (0.02)	Weißmair (2011)

Hundsalm Eis- und Tropfsteinhöhle (Brandenberg Alps)	1495				
HUN-H1		UBA-15860	326 ± 25	1485–1642 AD (1.00)	Spötl et al. (2014)
HUN-H2		UBA-15861	334 ± 25	1480–1640 AD (1.00)	Spötl et al. (2014)
HUN-H3		UBA-15862	38 ± 29	1695–1726 AD (0.19)	Spötl et al. (2014)
				1813–1838 AD (0.14)	
				1842–1853 AD (0.03)	
				1868–1918 AD (0.56)	
				1952–1955 AD (0.09)[c]	
HUN-H12		UBA-18582	250 ± 24	1528–1552 AD (0.06)	Spötl et al. (2014)
				1633–1669 AD (0.72)	
				1780–1798 AD (0.20)	
				1945–1951 AD (0.02)[c]	
HUN-H13		UBA-19071	800 ± 25	1189–1197 AD (0.02)	Spötl et al. (2014)
				1207–1274 AD (0.98)	
HUN-H14		UBA-19072	2664 ± 32	895–867 BC (0.14)	Spötl et al. (2014)
				863–795 BC (0.86)	
HUN-H16		UBA-20559	786 ± 31	1190–1196 AD (0.01)	Spötl et al. (2014)
				1207–1280 AD (0.99)	
HUN-H17		UBA-20560	790 ± 27	1210–1277 AD (1.00)	Spötl et al. (2014)
HUN-H18		UBA-21456	402 ± 29	1436–1521 AD (0.83)	Spötl et al. (2014)
				1575–1583 AD (0.01)	
				1590–1623 AD (0.15)	
HUN-H20		UBA-20561	1419 ± 30	582–661 AD (1.00)	Spötl et al. (2014)
HUN-H21		UBA-20710	1452 ± 30	560–650 AD (1.00)	Spötl et al. (2014)
HUN-H22		UBA-20888	361 ± 19	1455–1524 AD (0.56)	Spötl et al. (2014)
				1558–1564 AD (0.02)	
				1569–1631 AD (0.42)	
HUN-H25		UBA-21457	152 ± 29	1667–1708 AD (0.17)	Spötl et al. (2014)
				1718–1783 AD (0.34)	
				1796–1827 AD (0.12)	
				1832–1887 AD (0.18)	
				1911–1953 AD (0.19)[c]	

Continued

Table 13.1 Summary of Radiocarbon Dates of Organic Remains in East Alpine Ice Caves—cont'd

Cave (Mountain Range)	Elevation of Main Entrance (m a.s.l.)	Lab Code	Conventional ^{14}C Age BP	Calibrated ^{14}C Age (2 Sigma)[a]	Reference
HUN-H26		UBA-20889	688 ± 22	1272–1305 AD (0.78) 1364–1384 AD (0.22)	Spötl et al. (2014)
HUN-H27		UBA-21458	647 ± 32	1281–1328 AD (0.45) 1341–1395 AD (0.55)	Spötl et al. (2014)
HUN-H28		UBA-21459	172 ± 29	1660–1697 AD (0.18) 1725–1815 AD (0.55) 1835–1877 AD (0.07) 1917–1952 AD (0.20)[c]	Spötl et al. (2014)
HUN-H29		UBA-28124	333 ± 21	1485–1640 AD (1.00)	Spötl (unpubl.)
H-1		GrN-23952	1380 ± 30	607–680 AD (1.00)	Spötl et al. (2014)

[a] *Calibrated using CALIB 7.1 using the INTCAL13 database. Values in parentheses denote relative area under probability distribution.*
[b] Bone samples.
[c] Denotes influence of radiocarbon derived from nuclear testing.

13.6 OUTLOOK

Kern and Perșoiu (2013) made an attempt to compile historical data on ice volume change from caves in different parts of the world. For European ice caves, their data showed a decline of ice levels since about the middle of the 20th century and an acceleration of this trend in the 1980s. Observations from Austrian ice caves were not included in this compilation, but are generally consistent with these findings. A significant number of the 1200 caves hosting perennial ice, firn or snow in this mountainous country have either shown a strong decline in ice volume or a transition into a seasonal ice cave in recent decades. The larger the ice cave, the less prone they appear to be to the atmospheric warming trend of the 20th and 21st centuries, whose amplitude in the Alps is about twice the mean of the Northern Hemisphere (Auer et al., 2014). Some of the largest ice caves in Austria are also managed as show caves, and their meteorology and ice mass balance have been in part manipulated, e.g., by restricting the outflow of cold cave air during summer. Only scattered and discontinuous observations exist about Austrian ice caves prior to the 20th century (e.g., Fugger, 1888; Klappacher and Mais, 1999; Behm et al., 2009), but they consistently report markedly larger ice accumulations, reflecting the "glacier-friendly" climate of the Little Ice Age. Significant ice build-up during this period is also recorded by radiocarbon-dated organic remains in ice bodies from several East Alpine caves. These data also suggest generally small ice volumes during the preceding Medieval Warm Period and again positive mass balances during the Bronze Age. The emerging picture shows a broadly synchronous evolution of surface glaciers in the Alps (e.g., Holzhauser et al., 2005) and their counterparts in the subsurface of karstified mountains during the Holocene. Despite careful studies, none of the organic remains dates back to the first half of the Holocene, a time period when alpine glaciers were on average smaller than during the second half. Under current climate boundary conditions an increasing number of small- to medium-sized ice and firn bodies will likely disappear from East Alpine caves within the coming years. Only large caves at higher elevation and characterized by vigorous ventilation have a good chance to survive the next decades in spite of increasing winter temperatures.

ACKNOWLEDGMENTS

We are indebted to the following colleagues for providing photographs and data: Robbie Shone, Harald Zeitlhofer, Heiner Thaler, Helmuth Planer, Walter Klappacher, and Clemens Tenreiter.

REFERENCES

Abel, G., 1932. Die Feuertal-Eishöhle im Toten Gebirge und ihre Begehung. Der Bergfreund 5/6, 87–92.

Abel, G., 1965. Veränderungen am Höhleneis der Eisriesenwelt (Salzburg). Die Höhle 16, 105–106.

Achleitner, A., 1995. Zum Alter des Höhleneises in der Eisgruben-Eishöhle im Sarstein (Oberösterreich). Die Höhle 46, 1–5.

Auer, I., Foelsche, U., Böhm, R., Chimani, B., Haimberger, L., Kerschner, H., Koinig, K.A., Nicolussi, K., Spötl, C., 2014. Vergangene Klimaänderung in Österreich. In: Österreichischer Sachstandsbericht Klimawandel 2014 (AAR14). Austrian Panel on Climate Change (APCC). Austrian Academy of Sciences, Vienna, pp. 227–300.

Behm, M., Hausmann, H., 2007. Eisdickenmessungen in alpinen Höhlen mit Georadar. Die Höhle 58, 3–11.

Behm, M., Dittes, V., Greilinger, R., Hartmann, H., Plan, L., Sulzbacher, D., 2009. Decline of cave ice—a case study from the Austrian Alps (Europe) based on 416 years of observation. In: Proceedings 15th Int. Congr. Speleol., Kerrville, TX, July 19–26, 2009, vol. 3, pp. 1413–1416.

Behm, M., Plan, L., Seebacher, R., Buchegger, G., 2016. Dachstein. In: Spötl, C., Plan, L., Christian, E. (Eds.), Höhlen und Karst in Österreich. Oberösterreichisches Landesmuseum, Linz, pp. 569–588.
Bock, H., Lahner, G., Gaunersdorfer, G., 1913. Höhlen im Dachstein und ihre Bedeutung für die Geologie, Karsthydrographie und die Theorien über die Entstehung des Höhleneises. In: Verein für Höhlenkunde in Österreich, Graz. Reprint 2010 (Verein für Höhlenkunde Hallstatt-Obertraun).
Büntgen, U., Tegel, W., Nicolussi, W., McCormick, M., Frank, D., Trouet, V., Kaplan, J.O., Herzig, F., Heussner, K.-U., Wanner, H., Luterbacher, J., Esper, J., 2011. 2500 years of European climate variability and human susceptibility. Science 331, 578–582.
Fohlmeister, J., Vollweiler, N., Spötl, C., Mangini, A., 2013. COMNISPA II: update of a mid-European isotope climate record, 11 ka to present. The Holocene 23, 749–754.
Fritz, A., 1977. Pollenanalytische Untersuchungen von Alteisproben. Carnithia II 167/87, 217–226.
Fugger, E., 1888. Beobachtungen in den Eishöhlen des Untersberges bei Salzburg. Mitt. Ges. Salzburger Landeskunde 23, 1–99.
Fugger, E., 1891. Eishöhlen und Windröhren. Jahresbericht der k.k. Ober-Realschule in Salzburg 24, 1–70.
Fugger, E., 1892. Eishöhlen und Windröhren. Zweiter Theil. Jahresbericht der k.k. Ober-Realschule in Salzburg 25, 71–134.
Fugger, E., 1893. Eishöhlen und Windröhren. Dritter Theil (Schlus). Jahresbericht der k.k. Ober-Realschule in Salzburg 25, 135–223.
Geyer, E., Seebacher, R., Tenreiter, C., Knobloch, G., 2016. Totes Gebirge. In: Spötl, C., Plan, L., Christian, E. (Eds.), Höhlen und Karst in Österreich. Oberösterreichisches Landesmuseum, Linz, pp. 599–622.
Gressel, W., 1965. Veränderungen am Höhleneis der Eisriesenwelt (Salzburg). Die Höhle 16, 105–106.
Gruber, V., Ringer, W., Gräser, J., Aspek, W., Gschnaller, J., 2014. Comprehensive investigation of Radon exposure in Austrian tourist mines and caves. Radiat. Prot. Dosim. 162, 78–82.
Hartmann, H., Hartmann, W., 1984. Das Geldloch am Ötscher in Niederösterreich: Die Erforschungsgeschichte einer Höhle im Spiegel von vier Jahrhunderten. Die Höhle 35, 155–166.
Hauser, E., Oedl, R., 1926. Eisbildungen und meteorologische Beobachtungen. In: Angermayer, E., Asal, A., Czörnig-Czernhausen, W., Hauser, E., Lehmann, O., Oedl, R., Pia, J., Wettstein-Westersheim, O. (Eds.), Die Eisriesenwelt im Tennengebirge (Salzburg).—Speläologische Monographien. vol. 6. Speläol. Inst., Vienna, pp. 77–105.
Hausmann, H., Behm, M., 2011. Imaging the structure of cave ice by ground-penetrating radar. Cryosphere 5, 329–340.
Herrmann, E., 2017. Die Obstanser Eishöhle in den Karnischen Alpen, Osttirol. Die Höhle 68, 40–58.
Herrmann, E., Pucher, E., Nicolussi, K., 2010. Das Schneeloch auf der Hinteralm (Schneealpe, Steiermark): Speläomorphologie, Eisveränderung, Paläozoologie und Dendrochronologie. Die Höhle 61, 57–72.
Holzhauser, H., Magny, M., Zumbühl, H.J., 2005. Glacier and lake-level variations in west-central Europe over the last 3500 years. The Holocene 15, 789–801.
Ivy-Ochs, S., Kerschner, H., Maisch, M., Christl, M., Kubik, P.W., Schlüchter, C., 2009. Latest Pleistocene and Holocene glacier variations in the European Alps. Quat. Sci. Rev. 28, 2137–2149.
Jäger, V., 1919. Dr. Eberhard Fugger. Sein Werk. Mitt. Ges. Salzburger Landeskunde 59, 72–80.
Jansky, W., Tenreiter, C., Pürmayr, L., 2008. Das Feuertal-Höhlensystem als Teil des Schönberg-Höhlensystems. Die Höhle 59, 83–95.
Joerin, U.E., Nicolussi, K., Fischer, A., Stocker, T.F., Schlüchter, C., 2008. Holocene optimum events inferred from subglacial sediments at Tschierva glacier, eastern Swiss Alps. Quat. Sci. Rev. 27, 337–350.
Kern, Z., Perșoiu, A., 2013. Cave ice—the imminent loss of untapped mid-latitude cryospheric palaeoenvironmental archives. Quat. Sci. Rev. 67, 1–7.
Kern, Z., Fórizs, I., Pavuza, R., Molnar, M., Nagy, B., 2011. Isotope hydrological studies of the perennial ice deposit of Saarhalle, Mammuthöhle, Dachstein Mts, Austria. Cryosphere 5, 291–298.
Killian, K., 1935. Die Obstanser Eishöhle. Mitt. Höhlen- u. Karstforsch., 123–125.
Klappacher, W., 1996. Salzburger Höhlenbuch. vol. 6 Landesverein für Höhlenkunde, Salzburg.

Klappacher, W., Mais, K., 1999. Ice cave studies in Salzburg and the work of Eberhard Fugger 1842–1919. Slovesnsky Kras (Acta Carsologica Slovaca) 37, 115–130.
Kral, F., 1968. Pollenanalytische Untersuchungen zur Frage des Alters der Eisbildungen in der Dachstein-Rieseneishöhle. Die Höhle 19, 41–51.
Mais, K., Pavuza, R., 1999. Aktuelle höhlenklimatische Aspekte der Dachstein-Rieseneishöhle. Die Höhle 50, 126–140.
Mais, K., Pavuza, R., 2000. Hinweise zu Höhlenklima und Höhleneis in der Dachstein-Mammuthöhle (Oberösterreich). Die Höhle 51, 121–125.
Mais, K., Trimmel, H., 1992. 400 Jahre Forschung in den Höhlen des Ötschers (Niederösterreich). Die Höhle 43, 74–79.
Mangini, A., Spötl, C., Verdes, P., 2005. Reconstruction of temperature in the Central Alps during the past 2000 years from a $\delta^{18}O$ stalagmite record. Earth Planet. Sci. Lett. 235, 741–751.
May, B., Spötl, C., Wagenbach, D., Dublyansky, Y., Liebl, J., 2011. First investigations of an ice core from Eisriesenwelt cave (Austria). Cryosphere 5, 81–93.
Milius, J., Petters, C., 2012. Eisriesenwelt—from laser scanning to photo-realistic 3D model of the biggest ice cave on earth. In: Jekel, T., Car, A., Strobl, J., Griesebner, G. (Eds.), GI-Forum 2012: Geovisualisation, Society and Learning. Wichmann, Berlin, pp. 513–523.
Nicolussi, K., Patzelt, G., 2000. Untersuchungen zur holozänen Gletscherentwicklung von Pasterze und Gepatschferner (Ostalpen). Z. Gletscherk. Glazialgeol. 36, 1–87.
Obleitner, F., Spötl, C., 2011. The mass and energy balance of ice within the Eisriesenwelt cave Austria. Cryosphere 5, 245–257.
Pavuza, R., Mais, K., 1999. Aktuelle höhlenklimatische Aspekte der Dachstein-Rieseneishöhle. Die Höhle 50, 126–140.
Pavuza, R., Spötl, C., 2017. Neue Daten zu Vorkommen und Entstehung kryogener Calcite in ostalpinen Höhlen. Die Höhle 68, 100–106.
Petters, C., Milius, J., Buchroithner, M.F., 2011. Eisriesenwelt: terrestrial laser scanning and 3D visualisation of the largest ice cave on earth. In: Proceedings European LiDAR Mapping Forum, Salzburg, Austria. http://visual-geodata3d.com/img/Eisriesenwelt_Milius-Petters-Buchroithner_ELMF-2011.pdf.
Pillwein, E., 1919. Dr. Eberhard Fugger. Sein Leben.. Mit. Ges. Salzburger Landeskunde 59, 65–72.
Plan, L., Xaver, A., 2010. Geomorphologische Untersuchung und genetische Interpretation der Dachstein-Mammuthöhle (Österreich). Die Höhle 61, 18–38.
Pointner, P., Klappacher, W., 2016. Tennengebirge. In: Spötl, C., Plan, L., Christian, E. (Eds.), Höhlen und Karst in Österreich. Oberösterreichisches Landesmuseum, Linz, pp. 553–568.
Reitschuler, C., Schwarzenauer, T., Lins, P., Wagner, A.O., Spötl, C., Illmer, P., 2012. Zur Mikrobiologie von Bergmilch. Die Höhle 63, 3–17.
Reitschuler, C., Lins, P., Schwarzenauer, T., Spötl, C., Wagner, A.O., Illmer, P., 2015. New undescribed lineages of non-extremophilic archaea form a homogeneous and dominant element within alpine moonmilk microbiomes. Geomicrobiol. J. 32, 890–902.
Saar, R., 1955. Die Dachstein-Rieseneishöhle nächst Obertraun und ihre Funktion als dynamische Wetterhöhle. Jahrb. Oberösterr. Musealver. 100, 263–319.
Saar, R., 1956. Eishöhlen, ein meteorologisch-geophysikalisches Phänomen. Geogr. Ann. 38, 1–63.
Saar, R., Pirker, R., 1979. Geschichte der Höhlenforschung in Österreich. Die Höhle Beiheft 13, 1–96.
Sattler, B., Larch, P., Rambacher, J., Spötl, C., 2013. Das Eis der Hundsalm Eis- und Tropfsteinhöhle als Lebensraum für mikrobielle Gemeinschaften. Die Höhle 64, 15–24.
Schmeidl, H., Kral, F., 1969. Zur pollenanalytischen Altersbestimmung der Eisbildungen in der Schellenberger Eishöhle und in der Dachstein-Rieseneishöhle. Jahrb. Vereins zum Schutze der Alpenpflanzen und -tiere 34, 67–84.
Schöner, W., Weyss, G., Mursch-Radlgruber, E., 2011. Linkage of cave-ice changes to weather patterns inside and outside the cave Eisriesenwelt (Tennengebirge, Austria). Cryosphere 5, 603–616.
Spötl, C., 2008. Kryogene Karbonate im Höhleneis der Eisriesenwelt. Die Höhle 59, 26–36.

Spötl, C., 2013. Die Entdeckungsgeschichte und der ursprüngliche Zustand der Hundsalm Eis- und Tropfsteinhöhle. Höhlenkundliche Mitteilungen des Landesvereins für Höhlenkunde in Tirol 51, 22–33.
Spötl, C., Cheng, H., 2014. Holocene climate change, permafrost and cryogenic carbonate formation: insights from a recently deglaciated, high-elevation cave in the Austrian Alps. Clim. Past 10, 1349–1362.
Spötl, C., Reimer, P.J., Luetscher, M., 2014. Long-term mass balance of perennial firn and ice in an Alpine cave (Austria): constraints from radiocarbon-dated wood fragments. The Holocene 24, 165–175.
Spötl, C., Pavuza, R., 2016. Eishöhlen und Höhleneis. In: Spötl, C., Plan, L., Christian, E. (Eds.), Höhlen und Karst in Österreich. Oberösterreichisches Landesmuseum, Linz, pp. 139–154.
Spötl, C., Egger, M., Mangini, A., Pavuza, R., 2017. Das Karstsystem am Obstanser See (Kartitsch, Osttirol)—geowissenschaftliche Ergebnisse. Die Höhle 68, 59–78.
Thaler, K., 2008. Analyse der Temperaturverhältnisse in der Eisriesenwelt-Höhle im Tennengebirge anhand einer 12 jährigen Messreihe. Unpubl. MS thesis, Univ. Innsbruck.
Weißmair, R., 1995. Höhleneisbildung aus Schnee und Eisdynamik im Kraterschacht (Sengsengebirge, Oberösterreich). Die Höhle 46, 32–37.
Weißmair, R., 2011. Eisdatierung und Eisveränderungen im Kraterschacht (1651/24, Sengsengebirge, Oberösterreich) zwischen 1992 und 2009. Die Höhle 62, 27–30.
Wimmer, M., 2008. Eis- und Lufttemperaturmessungen im Schönberg-Höhlensystem (1626/300) und Modellvorstellungen über den Eiszyklus. Die Höhle 59, 13–25.
Zeitlhofer, H., Knobloch, G., 2008. Die Raucherkarhöhle (1626/55) als Teil des Schönberg-Höhlensystems. Die Höhle 59, 73–82.